First β-ν correlation measurement from the recoil-energy spectrum of Penning trapped ^{35}Ar ions

S. Van Gorp,[1,*] M. Breitenfeldt,[1] M. Tandecki,[1,†] M. Beck,[2,‡] P. Finlay,[1] P. Friedag,[2] F. Glück,[3,§] A. Herlert,[4,‖] V. Kozlov,[3] T. Porobic,[1] G. Soti,[1] E. Traykov,[1,¶] F. Wauters,[1,#] Ch. Weinheimer,[2] D. Zákoucký,[5] and N. Severijns[1]

[1]*Instituut voor Kern- en Stralingsfysica, K.U. Leuven, Celestijnenlaan 200D, B-3001 Leuven, Belgium*

[2]*Universität Münster, Institut für Kernphysik, Wilhelm-Klemm-Strasse 9, D-48149 Münster, Germany*

[3]*Karlsruhe Institute of Technology, Institut für Kernphysik, Postfach 3640, 76021 Karlsruhe, Germany*

[4]*University of Manchester, School of Physics and Astronomy, Manchester M13 9PL, United Kingdom*

[5]*Nuclear Physics Institute, ASCR, 250 68 Rež, Czech Republic*

(Received 25 March 2014; published 20 August 2014)

We demonstrate a novel method to search for physics beyond the standard model by determining the β-ν angular correlation from the recoil-ion energy distribution after β decay of ions stored in a Penning trap. This recoil-ion energy distribution is measured with a retardation spectrometer. The unique combination of the spectrometer with a Penning trap provides a number of advantages, e.g., a high recoil-ion count rate and low sensitivity to the initial position and velocity distribution of the ions and completely different sources of systematic errors compared to other state-of-the-art experiments. Results of a first measurement with the isotope ^{35}Ar are presented. Although currently at limited precision, we show that a statistical precision of about 0.5% is achievable with this unique method, thereby opening up the possibility of contributing to state-of-the-art searches for exotic currents in weak interactions.

DOI: 10.1103/PhysRevC.90.025502 PACS number(s): 23.40.Bw, 37.10.Ty, 37.10.Rs

I. INTRODUCTION

In recent years, ion and atom traps have been used for a wide range of applications in nuclear physics [1,2], including precision measurements for the study of fundamental interactions [3,4]. The conditions offered by particle traps are ideal to reduce instrumental effects in β-decay measurements, in particular the scattering or absorption of β particles, which is a limiting factor when radioactive sources are embedded in material [5,6]. In addition, they enable the direct detection of recoil ions from β decay, which typically have kinetic energies below 1 keV. These advantages have already led to several high-precision measurements of angular correlation coefficients in β decay [7–12] searching for exotic scalar or tensor type weak interactions beyond the standard electroweak model [3,13–15] that would induce small shifts in the values of experimental observables. The possible presence of such new interactions would imply the existence of corresponding mediator bosons, particles which are searched for directly with the Large Hadron Collider (see, e.g., Refs. [16–18]).

Most of these experiments observe coincidences between the β particle and the recoiling daughter nucleus. The Weak Interaction Trap for Charged Particles (WITCH) experiment [19–23] at ISOLDE/CERN applies a unique method; i.e., it uses a double Penning trap system to prepare the source for the experiment and a retardation spectrometer to measure the recoil-ion energy distribution as shown in Fig. 1. Unlike laser-based atom traps, Penning traps are not element selective and can thus be used for a large variety of isotopes. State-of-the-art experiments with a magneto-optical trap or Paul trap are limited by the available space to place particle detectors (used in coincidence), which is no issue in a Penning trap since the magnetic field focuses 50% of the recoil ions to the detector which is 2.7 m downstream.

The shape of the measured retardation spectrum depends on the β-ν correlation coefficient a [24], which is highly sensitive to the presence of charged weak currents beyond the standard model (SM) [3,15]. The parameter that is actually being determined in this experiment is not a, but

$$\tilde{a} = \frac{a}{1+b'}, \tag{1}$$

with

$$b' \simeq \pm\frac{\gamma m}{E_e}\frac{1}{1+\rho^2}\left[\mathrm{Re}\left(\frac{C_S+C_S'}{C_V}\right)+\rho^2\mathrm{Re}\left(\frac{C_T+C_T'}{C_A}\right)\right], \tag{2}$$

with $\gamma=\sqrt{(1-\alpha^2Z^2)}$, α the fine-structure constant, Z the charge of the daughter nucleus, m the electron mass, E_e the total β-particle energy, and $C_S, C_S', C_T, C_T', C_V, C_V', C_A, C_A'$ the coupling constants for scalar (S), tensor (T), vector (V), and axial vector (A) types of weak interaction [15], respectively,

*Present address: Atomic Physics Laboratory, RIKEN, Saitama 351-0198, Japan; simonvgorp@gmail.com

†Present address: TRIUMF, 4004 Wesbrook Mall, Vancouver, British Columbia, Canada V6T 2A3.

‡Present address: Johannes Gutenberg Universität Mainz, Institute of Physics, Staudingerweg 7, D-55128 Mainz, Germany.

§Present address: Wigner Research Institute for Physics, 1525 Budapest, POB 49, Hungary.

‖Present address: FAIR, Planckstrasse 1, 64291 Darmstadt, Germany.

¶Present address: GANIL, CEA/DSM-CNRS/IN2P3, Caen, France.

#Present address: University of Washington, Seattle, WA 98195, USA.

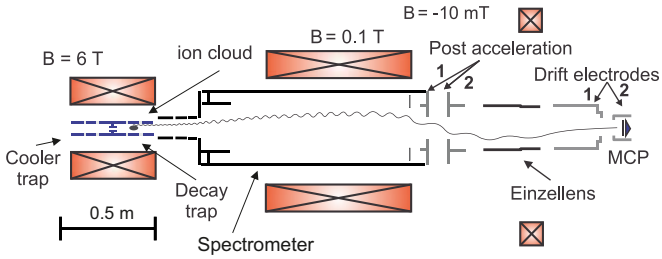

FIG. 1. (Color online) Scheme of the WITCH Penning traps and the spectrometer with an example trajectory of a recoil ion from the traps to the detector. For a figure of the complete setup see, e.g., Ref. [23].

while

$$a \simeq a_{\mathrm{SM}} - \frac{1}{(1+\rho^2)^2}\left[\left(1+\frac{1}{3}\rho^2\right)\frac{|C_S|^2+|C_S'|^2}{C_V^2} + \frac{1}{3}\rho^2(1-\rho^2)\frac{|C_T|^2+|C_T'|^2}{C_A^2}\right], \quad (3)$$

with

$$a_{\mathrm{SM}} = \frac{1-\rho^2/3}{1+\rho^2}, \quad (4)$$

and ρ the Gamow-Teller (GT)-Fermi mixing ratio

$$\rho = \frac{C_A M_{\mathrm{GT}}}{C_V M_F}. \quad (5)$$

In Fermi β decay $a = +1$ for a pure vector interaction while $a = -1$ for a pure scalar interaction. For ^{35}Ar the mixing ratio $\rho = -0.2841(25)$ so that $a_{\mathrm{SM}} = 0.900(2)$ [25], rendering its measurement mainly sensitive to scalar charged weak currents.

The advantages of this novel setup are threefold: the magnetic field focuses almost half of the recoil ions toward the microchannel plate (MCP) detector resulting in a high recoil-ion count rate, a retardation spectrometer has a low sensitivity to the source parameters, and the error budget is different compared to state-of-the-art experiments, which is important to establish or put constraints on the existence of exotic currents. In this paper we report on the first measurement of the recoil-ion energy spectrum of ^{35}Ar using a Penning ion trap, we discuss the analysis procedure which includes extensive simulations, and we demonstrate how the β-ν correlation coefficient is extracted. We show that most of the systematic uncertainties of the experiment are under control and how the remaining ones can be improved. Altogether we demonstrate that this novel technique is competitive with current best experiments since a statistical precision on a of about 0.5% or better can be reached.

II. EXPERIMENT

The isotope ^{35}Ar was chosen as its SM value for a can be calculated with per mil precision [25]. Furthermore, the ^{35}Ar half-life of $T_{1/2} = 1.775(4)$ s represents a good trade-off between the preparation of the sample in the Penning trap and the collection of statistics through its β decay. ^{35}Ar is also produced in large quantities at ISOLDE [26] (2.0×10^8 ions/μC [27]), and nuclear structure-related effects are well known for their superallowed mirror decay [25]. Finally it has a stable daughter isotope and a simple decay scheme. Previously, the β-ν angular correlation coefficient of ^{35}Ar was obtained from a measurement of the recoil energy distribution with radioactive argon gas and two 10-cm-long electrostatic spectrometers [28]. This resulted in the value $a = 0.97 \pm 0.14$, limited mainly by the unknown charge state distribution of the recoiling ions.

In the experiment described here, the $^{35}Ar^{1+}$ ions are produced at ISOLDE by bombarding a CaO target with a 1.4-GeV proton beam and using a plasma ion source with a cold transfer line. The continuous 30-keV beam is bunched in the REXTRAP Penning trap [29] and subsequently transferred to the WITCH setup, where its energy is brought down to about 200 eV using a pulsed drift tube (PDT) [30]. This allows capturing the ions in the cooler trap, which is the first of two sequential Penning traps. Ions are cooled for 0.5 s by the combination of buffer-gas collisions and a quadrupolar rf excitation on the mass-specific cyclotron frequency. Cooled ions are transferred to the decay Penning trap and subsequently kept there for 1.5 s in a quadrupole potential with a depth of 5 V (see below) and left to decay. Because the recoil-ion energy for the ^{35}Cl daughter ions ranges up to 452 eV, most recoil ions can easily overcome this potential barrier. At the end of each 2-s cycle the decay trap is emptied by ejecting any remaining ions backward.

The total energy of the recoil ions is probed with a retardation spectrometer of the MAC-E filter type [31,32] (see Fig. 1), blocking all ions with a recoil energy too low to overcome the applied potential. With a 6-T magnetic field in the Penning trap region and 0.1 T in the retardation region, 98.3% of an ion's radial energy is converted into axial energy such that in the retardation plane nearly the total recoil energy is probed. By varying the barrier voltage, the integral recoil energy spectrum is obtained. Ions that pass the analysis plane are pulled off the magnetic field lines by a negative electric potential of a few kilovolts. An Einzel lens and two drift electrodes focus these ions onto the Roentdek MCP detector with an active radius of 41.5 mm [33–35]. The MCP's position sensitivity allows to measure the radial distribution of the recoiling ions, providing additional information of the ion cloud properties in the decay trap. Note that during the experiment discussed in this paper some electrodes in the drift section and postacceleration section were not ramped to the nominal values to prevent sparks and unwanted discharges, causing a nonoptimal focus of the ions. These technical issues have meanwhile been solved.

A superior advantage of combining the strength of Penning traps with a retardation spectrometer is a high count rate since the magnetic field focuses almost 50% of the recoiling ions onto the detector. Furthermore, there is no large dependence on the position distribution since almost all of these ions are focused on the MCP detector. The ion cloud also has a thermal energy distribution leading to minimal Doppler broadening. Additionally both the radial and total energy distributions of the cloud can be measured to high precision and can therefore be taken into account in the analysis.

With $^{35}Ar^{1+}$ decaying via a β^+ transition, the larger fraction of the ^{35}Cl daughter nuclei, i.e., 72(10)% [36], are neutral and therefore escape detection. The electron shake-off process further generates charge states up to 4^+ and higher. This charge-state distribution (CSD) after β^+ decay of $^{35}Ar^+$ ions was measured with the LPCTrap setup at GANIL, showing that 75(1)%, 17.2(4)%, 5.7(3)%, 1.6(2)%, and 0.7(2)% of the charged recoil ions end up in the 1^+, 2^+, 3^+, 4^+, and higher charge states, respectively [36].

A. Technical improvements

Previously we already demonstrated the measurement of a recoil-ion spectrum with the WITCH setup using ^{124}In ions [21]. However, the β-ν angular correlation coefficient that can be extracted from the recoil ion spectrum of ^{124}In ions is difficult to interpret due to the complex decay scheme of this isotope and therefore does not allow extracting information on physics beyond the standard model. For a sensitive measurement with the preferred isotope ^{35}Ar several technical improvements were required and implemented.

First, the ^{35}Ar beam from ISOLDE was found to be contaminated with stable ^{35}Cl ions (ratio 1:100). Mass separation of both species was not possible in the WITCH cooler trap nor in REXTRAP due to the too-high chlorine contamination and the large number of ions involved (1×10^5). The development of a nanostructured CaO target and a different target cleaning procedure reduced the amount of chlorine atoms to a negligible level while achieving a greater yield of ^{35}Ar ions [27].

Since argon is a noble gas, trapped ^{35}Ar ions have a strong tendency to charge exchange. The charge-exchange half-life was determined to be 8 ms in the WITCH cooler trap and 75 ms in REXTRAP. Therefore, the Teflon buffer-gas system was replaced with an all-metal system and a nonevaporable getter (NEG) pump was installed in the buffer-gas line. A recent measurement with stable argon showed that there are no losses in the decay trap for up to 10 s.

The combination of magnetic and electric fields in the spectrometer can lead to unwanted (Penning) traps for charged particles in the system. Therefore, field emission points from electrodes were rounded and electrodes electropolished. Furthermore, the number of background gas atoms was reduced by removing materials with a high outgassing rate (e.g., Teflon) and adding pumping capacity (e.g., NEG coatings inside the system). An additional coil producing a compensating magnetic field of 10 mT was installed to break the trap in the Einzel lens region (see Fig. 1) and a wire was added in the spectrometer region to remove the electrons that accumulate there. These improvements allowed the electrodes to operate at higher voltages and thus enabled the spectrometer to probe the recoil-ion energy, which was not possible in the experiment described in Ref. [21] when the Einzel lens electrode was used for this purpose.

Off-line tests of the WITCH setup were made possible with the development of a modular control system for the experiment [37] and a compact (15-cm-long) radio frequency quadrupole and ion source [38]. The implementation of all these technical developments and the creation of simulation codes have allowed the first determination of a on ^{35}Ar with the WITCH setup, which is described in this paper.

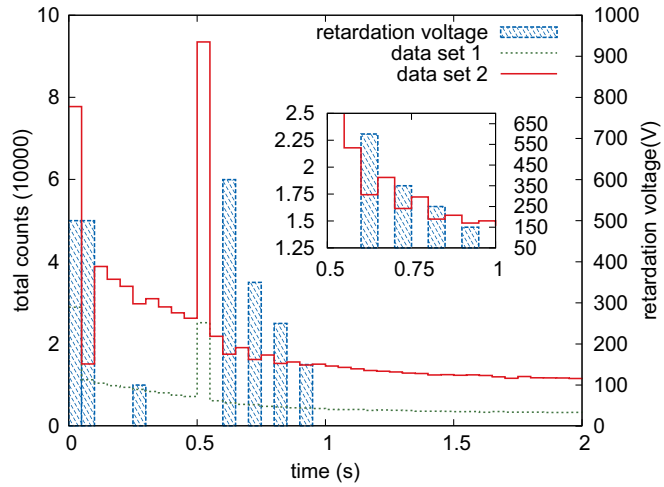

FIG. 2. (Color online) Overview of the two data sets obtained in this experiment. Data set 1 (bottom, dashed curve) is the sum of all cycles with no retardation barrier applied. Data set 2 (top, solid curve) is the sum of all cycles with retardation voltages applied in some of the time bins (inset zoomed). The argon ions are kept in the cooler trap from $t = 0$ s until $t = 0.5$ s and in the decay trap from $t = 0.5$ s until $t = 2$ s.

B. Acquired data set

Figure 2 displays the raw counts obtained from the decay of ^{35}Ar ions in the decay trap. First, data were collected without retardation voltage; i.e., all recoil ions escaping from the decay trap were collected (called "data set 1"). This data set was used for the normalization. Subsequently, the measurement was repeated with a retardation voltage being applied in several time bins during the first 1 s of each cycle in order to measure the recoil energy distribution (called "data set 2"). Significantly more counts are observed in both data sets at $t = 0$ s, which is due to ions too energetic to be captured in the cooler trap which are thus passing through. Similarly, ions that cannot be captured in the decay trap when being transferred from the cooler trap to the decay trap are observed at $t = 0.50$ s.

The pulse height distribution (PHD) of MCP signals is a characteristic of the particles detected, i.e., a sharp rise followed by an exponential drop in counts for β particles and dark counts, and a bell-like (Gaussian) shape for ions [33]. This feature was used to confirm that the particles that were blocked by the retardation voltages were indeed ions (Fig. 3). The amount of ions stored in the decay trap in each cycle was estimated from the difference in counts collected in the time bins at $t = 0.55$ s (no blocking voltage) and $t = 0.60$ s (all ions blocked), duly correcting for dead time and taking into account the different efficiencies involved, resulting in 2600 ± 900 ions. With this number of ions, space charge-related effects [39,40] are still limited.

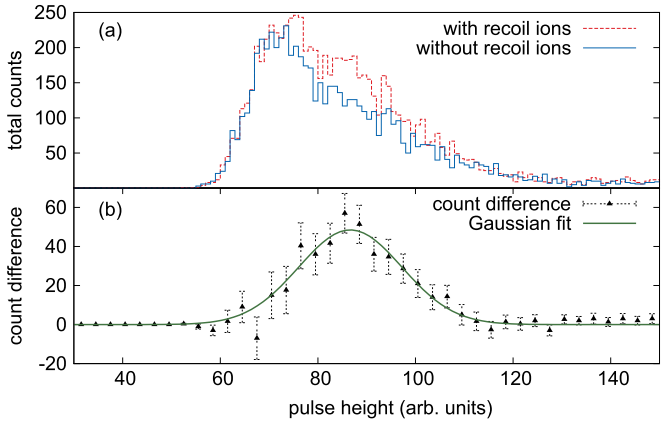

FIG. 3. (Color online) (a) PHD of particles arriving on the MCP detector, without retardation voltage, i.e., with recoil ions ($t = 0.55$ s), and with 600 V ($t = 0.60$ s) being applied, which blocks all recoil ions. (b) Rebinned difference in counts for the two PHDs in the upper panel with statistical error bars and a Gaussian fit ($\chi^2/\nu = 0.7$), which is typical for ions.

III. ANALYSIS

The recoil-energy spectrum was obtained by subtracting data sets 1 and 2 shown in Fig. 2. Both data sets were normalized by comparing the points where no retardation voltage was applied. The corresponding scaling factor $f = 3.540(3)$ was determined using a regression analysis. The statistical uncertainties related to this have been taken into account by error propagation. The resulting spectrum is displayed in Fig. 4 together with the final spectrum after correcting for the half-life of ^{35}Ar and losses in the decay trap. These losses were found to be related to nonoptimal values for the trap timings and voltages applied during the experiment. To quantify the losses, a calibration measurement was performed with stable $^{39}K^{1+}$ ions for identical settings.

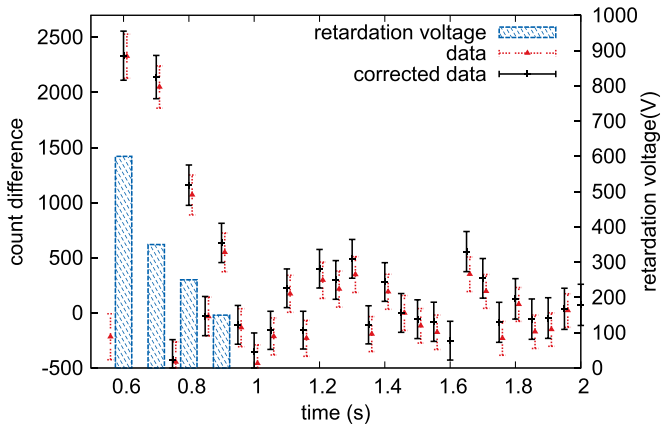

FIG. 4. (Color online) Difference in counts between data set 2 (obtained with retardation voltages applied) and the scaled data set 1 (without retardation voltages applied). Raw data and the data corrected for the ^{35}Ar half-life and losses in the decay trap; see text for details.

A. Simulations

Two simulation codes were used in the data analysis. The SIMBUCA simulation package [41] models the behavior of multiple ions in a Penning trap and is used to obtain the position and velocity distributions of ions stored in the decay trap. The simulated position and velocity distributions for the ion cloud in the decay trap are subsequently used as input for the SIMWITCH program [35], which is based on Ref. [42] and performs the tracking of the particle through the entire setup and up to the position-sensitive MCP detector (Fig. 1).

1. SIMBUCA simulation package

The SIMBUCA code can handle rf excitations of the ion motion, electric and magnetic field maps, buffer-gas collisions and Coulomb interactions between ions. Using a graphics card (GPU) for the latter dramatically reduces the simulation time [41]. The simulations for the analysis presented here were performed for a cloud consisting of 2600 $^{35}Ar^{+}$ ions. The ion cloud properties are simulated for the entire duration of the experimental cycle, i.e., from the capture and compression ($\nu_c = 2.634374$ MHz, amplitude 2.4 V) of the ions in the cooler trap until their transfer to and storage in the decay trap. To take into account the actual experimental settings, the COMSOL [43] package was used to calculate the electrical field map, while the magnetic field map was provided by Oxford Instruments.

The simulations with SIMBUCA show that with a quadrupolar rf excitation being applied for 500 ms while the ions are in the cooler trap, all ions are cooled down to room temperature, i.e., 0.025 eV. At the same time the radial position distribution with a full width at half maximum of 6 mm (with which the ions arrive in the cooler trap after having been pulsed down in energy from 30 keV to a few hundred eV in the PDT [30]) is reduced to 0.1 mm. An optimal transfer of the ion cloud from the cooler trap to the decay trap does not provide the ions with additional energy nor does it influence the spatial distribution. During the experiment described here the duration for this transfer was tuned to be 31.5 μs. However, simulations show that for the trap settings used this transfer time was too short and should have been 38.5 μs. Simulations further reveal that due to this too-short transfer time the argon ions are heated after the transfer to a maximum energy of 4.5 eV (instead of 0.1 eV for an optimal transfer). This simulated maximum ion energy is in perfect agreement with the experimentally optimized potential depth of 5 V in the decay trap, which was obtained by increasing the voltage in 1-V steps until no ions were evaporating from the trap anymore. Table I shows the resulting position and velocity distributions of the cloud in the decay trap, assuming a Gaussian distribution. The SIMBUCA package was validated by simulating a radially outward drifting ion that is subject to a dipolar excitation. Perfect agreement between the simulated and theoretically expected ion trajectory was found [41]. Furthermore, aside from comparing SIMBUCA to an analytical solution the code was also tested by additional offline experiments. In one of these N $^{39}K^{1+}$ ions were accumulated in the buffer-gas-filled cooler trap (pressure 2.4×10^{-2} mbar). Afterward a quadrupole excitation was applied with the cyclotron frequency ν_c. It is known that for a

TABLE I. Overview of the simulated Gaussian position and velocity distribution in the decay trap for the settings as applied during the experiment (first column) and for the optimal settings when a perfect transfer between the traps is assumed.

	Expt. settings		Optimal settings	
	μ	σ	μ	σ
x, y (cm)	0	5.0×10^{-3}	0	3.3×10^{-3}
z (cm)	0.032	2.8	0	0.4
$v_{x,y}$ (m/s)	−0.2	460	0	386
v_z (m/s)	−5	3290	0	424

single ion in the trap ($N = 1$) the excitation cools and centers the particle [44]. However, it is experimentally observed that if $N > 1$ the optimal excitation frequency will shift to higher values [29,39]. The experiment was performed by varying N between 30.000 and 175.000 and the optimal centering frequency ν_{rf} was determined. It was found that $\Delta\nu = \nu_{\mathrm{rf}} - \nu_c$ scales linearly with N and ranges between 200 and 1200 Hz [40]. These experimental conditions were reproduced in SIMBUCA, requiring the electric field map from COMSOL, the magnetic field map from the magnet manufacturer, the estimated buffer-gas pressure in the trap (from the gauge readout), and the application of a quadrupole excitation. These simulations showed exactly the same scaling of $\Delta\nu$ [40].

2. *SIMWITCH simulation package*

SIMWITCH adds a recoil energy randomly picked from the theoretical distribution for $a = \pm1$ to the recoiling daughter ion and then tracks it from its creation in the ion cloud in the decay trap, through the spectrometer, and up to its arrival on the MCP detector or its loss in the system, thereby taking into account the electromagnetic field configuration. The particle tracking includes various effects like velocity Doppler broadening and losses due to nonoptimal field configurations. SIMWITCH simulations were performed for the different retardation voltages used in the experiment (i.e., 0, 150, 250, 350, and 600 V) and for 1^+ up to 5^+ charge states. These showed that, due to the nonoptimal electrode settings in the spectrometer, 54% of the recoil ions are lost when they hit the drift electrodes.

Every part of the SIMWITCH code was tested separately. This includes the randomization of the recoil-energy distribution, the effect of the charge state, as well as the tracking in the presence of electric and magnetic fields. The validity of SIMWITCH was further verified by comparing the theoretical cutoff angle (i.e., the maximum emission angle with respect to the magnetic field axis for which recoil ions can still be transported into the retardation spectrometer; see Fig. 1) and the simulated one. The difference of a few percent is considered to be due to a limited analytical model, which is currently being improved [35].

B. Results

The recoil-ion energy distribution, obtained as the difference in counts on the MCP detector for the different retardation voltages applied (see Fig. 4), is shown in Fig. 5. Since the recoil-energy spectrum is linear in a [24], the β-ν angular correlation coefficient a can be extracted from this by comparing the experimental data, $f(a)$, with a linear combination of the simulated results, $g(a)$, for $a = \pm1$, with the correlation coefficient a and amplitude A as fit parameters:

$$f(a) = A\left[\frac{1-a}{2}g(a=+1) + \frac{1+a}{2}g(a=-1)\right]. \quad (6)$$

This yielded $a = 1.12 \pm 0.33_{\mathrm{stat}}$ with $\chi^2/\nu = 0.64$ as indicated by the solid line in Fig. 5 and agrees with the standard model value $a = 0.900(2)$ [25].

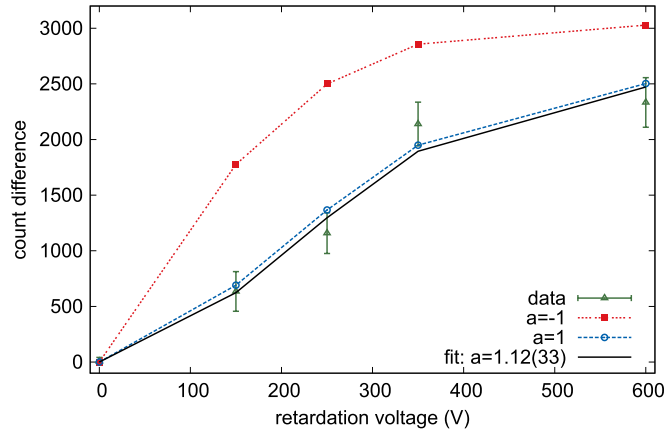

FIG. 5. (Color online) Recoil-ion energy spectrum for ^{35}Cl daughter ions. The black line corresponds to the best fit to the data, yielding $a = 1.12 \pm 0.33_{\mathrm{stat}}$. For comparison the curves simulated for $a = +1$ (pure vector interaction) and $a = -1$ (pure scalar interaction) are also shown. The SM value is $a = 0.900(2)$ [25]. Lines are drawn to guide the eye.

C. Systematic uncertainties

Systematic effects from the measured β-ν angular correlation coefficient can have two origins. They propagate either through the reconstructed data or through the simulated data for $a = 1$ and $a = -1$. In the first case systematic errors stem from the limited precision of the half-life of ^{35}Ar and from the limited precision of the trap-loss rate which were both taken into account via error propagation. Systematic errors in the SIMBUCA and SIMWITCH simulation codes can originate from using an inaccurate experimental description of the apparatus (e.g., electrode dimensions) or from the limited precision on the input parameters (e.g., the charge-state distribution). The systematic error induced by SIMWITCH originates from uncertainties on the electrode dimensions, on the magnetic field strength, and on the applied potentials. SIMBUCA, ultimately, induces a rather limited systematic error since the properties of the cloud in the decay trap can in principle be determined to arbitrary precision given sufficient measurement time. Indeed, the total and axial energy distribution of the trapped particles can be measured experimentally by respectively lowering the potential barrier of the analysis plane or the potential on the upstream end cap of the decay trap and each time count the number of ions that reach an MCP in the analysis plane.

TABLE II. List of leading systematic effects (see also Ref. [45]). The second column indicates by how much a certain parameter may vary to induce either a shift of 0.5% in the value of a or a systematic uncertainty of 0.5% on a. The last column indicates how well the parameter is currently under control.

Systematic effect	0.5%	Current control
Precision on half-life (s)	0.005	0.001
Variation in surface potential (V)	0.2	0.5
Precision on retardation potential (%)	2.5	0.1
Ion cloud mean energy (eV)	$\approx$0.1	$\approx$0.05
Precision of magnetic field ratio (%)	$\approx$10	$\ll$0.1
Precision on 1-V end cap potential (%)	40	1
Space-charge potential (no. ions)	$\approx 1\times10^6$	$\approx 1.2\times10^5$
Error on fraction of 1^+, 2^+, 3^+, 4^+, $>4^+$ in the CSD (%)	0.6, 1, 3, 11, 20	1.4, 2.6, 4.7, 13.3, 24.4[a]
1^+, 2^+, 3^+ CSD dependence on recoil energy (%)		0.1, 0.23, 0.04[a]

[a]Reference [36].

Furthermore, the cloud's radial position distribution can be determined by ejecting the cloud in the decay trap on the position-sensitive MCP detector (see Fig. 1). The number of particles, N, in the cloud can be obtained, for example, from the number of measured β particles. Finally the axial length and density of the cloud can be calculated given N, the radial length, and the shape of the potential. The properties of the ion cloud in the decay trap can thus be characterized rather precisely such that SIMBUCA simulations might in the future not even be required anymore since the measured position and velocity distribution can be fed directly to the SIMWITCH simulations.

Table II summarizes all systematic effects, their required precision for a measurement on a below 0.5%, and the currently known precision. Two additional systematic effects are currently being quantified. The first effect relates to the wire in the analysis plane of the spectrometer [35]. This wire was introduced to break the storage condition for electrons since the magnetic field and electrical potentials of the WITCH spectrometer form an unwanted Penning trap for electrons and the magnetic drift of stored electrons will let them hit the wire after a short time. This wire shifts the potential in the analysis plane between 0.8% (for a 100-V retardation barrier) and 0.5% (400-V retardation barrier). The effect of this on a is taken into account with the three-dimensional field map of SIMWITCH. The spatial position and dimensions of the wire were carefully measured so as to limit the corresponding systematic effect on a below 0.5%.

The second effect is a fluctuating background level due to unwanted secondary ionization and discharges, which is an inherent challenge with spectrometers. This background has been significantly reduced already by improving the vacuum in the system, purifying the buffer gas, and installing the wire in the spectrometer. Nevertheless, in the data presented here the background level, which was observed when the spectrometer was set to 0 V, still showed a sudden increase up to at most double the normal intensity in about 20% of the cycles. Data from these cycles were left out of the analysis. To quantify the effect of the fluctuating background the influence of variables like rest-gas pressure and spectrometer voltages is being studied.

As can be seen from Table II, the leading systematic effects are currently under control. The required MCP surface efficiency (an efficiency variation smaller than 2% at 95% confidence level is expected [33]) for a high-precision experiment is at present under investigation. However, the MCP surface efficiency will be measured after (and before) the experiment and can be used to correct the data. Ongoing data analysis of the LPCTrap experiment will further reduce the error on the CSD fractions by at least a factor of 4 [46], reducing this systematic uncertainty to a negligible level for the WITCH experiment. At present the attainable precision is thus limited by the surface potential on the electrodes. This variation in surface potential can be improved by using, for example, galvanically deposited gold layers on the trap electrodes, which will reduce the work function fluctuations to 30–40 meV rms [47].

IV. CONCLUSION AND OUTLOOK

We presented a novel technique that combines a Penning trap with a retardation spectrometer to search for physics beyond the standard model. The benefits of this method are a high count rate, low sensitivity to the source parameters, and completely different sources of systematic errors than current state-of-the-art experiments. In addition, the procedure for analysis of such data was developed and applied, including the validation and use of two simulation codes, one to determine the position and velocity distribution of the ions in the Penning trap (which in the future will be obtained with good precision from direct measurements) and a second one to track the recoil ions through the retardation spectrometer onto the position-sensitive MCP detector. A first result for the β-ν correlation coefficient a for ^{35}Ar was extracted and the leading systematic effects were discussed.

The measurement discussed here can be further optimized to increase the amount of recoil ions counted. As listed in Table III, an increase in statistics by a factor of about 8000 is possible, bringing down the statistical error to below 0.5% and allowing a competitive determination of the β-ν angular correlation coefficient, a. Since the completion of the presented analysis the efficiency of the beam transport, injection into the magnetic field, and focus of the spectrometer electrodes have been improved by a factor of 10, 2, and 2, respectively.

TABLE III. List of possible improvements and the corresponding gain factor.

Improvement	Gain
Transport efficiency from ISOLDE to WITCH	20
Injection efficiency into WITCH magnetic field	4
Optimal spectrometer settings to focus all ions	2
100 h measurement time instead of 4 h	25
Measurement cycle of 1.5 s instead of 0.5 s	2
Total gain	8000

Together with anticipated longer measuring and cycle times this results in a factor-of-2000 improvement in counting statistics.

Although the current result is not yet competitive, the proof of principle of this novel technique is an important milestone toward the search for physics beyond the standard model.

ACKNOWLEDGMENTS

We thank the ISOLDE Collaboration and the ISOLDE operators. This work was supported by FWO-Vlaanderen (Belgium), GOA/2010/10 (BOF-K.U.Leuven), IUAP—Belgian State Belgian Science Policy (BriX network P6/23), German BMBF-Verbundforschung (Foederkennzeichen 06MS9151I), Grants No. LA08015 and No. LG13031 of the Ministry of Education of the Czech Republic, and by the European Commission within the Framework Program through I3-EURONS (Contract No. RII3-CT-2004-506065) and I3-ENSAR (Project No. 262010).

[1] K. Blaum, Phys. Rep. **425**, 1 (2006).
[2] H. J. Kluge, Nucl. Phys. A **701**, 495 (2002).
[3] N. Severijns *et al.*, Rev. Mod. Phys. **78**, 991 (2006).
[4] J. A. Behr and G. Gwinner, J. Phys. G: Nucl. Part. Phys. **36**, 033101 (2009).
[5] F. Wauters *et al.*, Phys. Rev. C **80**, 062501(R) (2009).
[6] F. Wauters *et al.*, Phys. Rev. C **82**, 055502 (2010).
[7] P. A. Vetter, J. R. Abo-Shaeer, S. J. Freedman, and R. Maruyama, Phys. Rev. C **77**, 035502 (2008).
[8] A. Gorelov *et al.*, Phys. Rev. Lett. **94**, 142501 (2005).
[9] X. Fléchard, Ph. Velten, E. Liénard, A. Méry, D Rodríguez, G. Ban, D. Durand, F. Mauger, O. Naviliat-Cuncic, and J. C. Thomas, J. Phys. G: Nucl. Part. Phys. **38**, 055101 (2011).
[10] E. G. Adelberger *et al.* (ISOLDE Collaboration), Phys. Rev. Lett. **83**, 1299 (1999); **83**, 3101(E) (1999).
[11] J. Pitcairn *et al.*, Phys. Rev. C **79**, 015501 (2009).
[12] D. Melconian *et al.*, Phys. Lett. B **649**, 370 (2007).
[13] N. Severijns and O. Naviliat-Cuncic, Annu. Rev. Nucl. Part. Sci. **61**, 23 (2011).
[14] F. Wauters, A. Garciá, and R. Hong, Phys. Rev. C **89**, 025501 (2014).
[15] J. D. Jackson *et al.*, Nucl. Phys. **4**, 206 (1957).
[16] O. Naviliat-Cuncic and M. González-Alonso, Ann. Phys. (Berlin) **525**, 600 (2013)
[17] T. Bhattacharya, V. Cirigliano, S. D. Cohen, A. Filipuzzi, M. Gonzalez-Alonso, M. L. Graesser, R. Gupta, and H.-W. Lin, Phys. Rev. D **85**, 054512 (2012).
[18] V. Cirigliano *et al.*, Prog. Part. Nucl. Phys. **71**, 93 (2013).
[19] B. Delauré, M. Beck, V. V. Golovko, V. Kozlov, T. Phalet, P. Schuurmans, N. Severijns, B. Vereecke, S. Versyck, D. Beck, W. Quint, F. Ames, K. Reisinger, O. Forstner, J. Deutsch, G. Bollen, and S. Schwarz, Hyperfine Interact. **146**, 91 (2003).
[20] M. Beck *et al.*, Nucl. Instrum. Methods Phys. Res. Sect. A **503**, 567 (2003).
[21] V. Yu. Kozlov, M. Beckb, S. Coecka, P. Delahayec, P. Friedagb, M. Herbanea, A. Herlertc, I. S. Kraeva, M. Tandeckia, S. Van Gorpa, F. Wautersa, Ch. Weinheimerb, F. Wenanderc, D. Zákouckýd, and N. Severijns, Nucl. Instrum. Methods Phys. Res. Sect. B **226**, 4515 (2008).
[22] V. Yu. Kozlov, M. Beck, S. Coeck, M. Herbane, I. S. Kraev, N. Severijns, F. Wauters, P. Delahaye, A. Herlert, F. Wenander, and D. Zákoucký, Hyperfine Interact. **172**, 15 (2006).
[23] M. Beck *et al.*, Eur. Phys. J. A **47**, 45 (2011).
[24] O. Kofoed-Hansen, Mat. Fys. Medd. K. Dan. Vidensk. Selsk. **28**, 1 (1954).
[25] N. Severijns, M. Tandecki, T. Phalet, and I. S. Towner, Phys. Rev. C **78**, 055501 (2008).
[26] E. Kugler, Hyperfine Interact. **129**, 23 (2000).
[27] J. P. Ramos *et al.*, Nucl. Instrum. Methods Phys. Res. Sect. B **320**, 83 (2014).
[28] J. S. Allen *et al.*, Phys. Rev. **116**, 134 (1959).
[29] F. Ames *et al.*, Nucl. Instrum. Methods Phys. Res. Sect. A **538**, 17 (2005).
[30] S. Coeck *et al.*, Nucl. Instrum. Methods Phys. Res. Sect. A **572**, 585 (2007).
[31] V. M. Lobashev and P. E. Spivak, Nucl. Instrum. Methods Phys. Res. Sect. A **240**, 305 (1985).
[32] A. Picard *et al.*, Nucl. Instrum. Methods Phys. Res. Sect. B **63**, 345 (1992).
[33] E. Liénard *et al.*, Nucl. Instrum. Methods Phys. Res. Sect. A **551**, 375 (2005).
[34] S. Coeck *et al.*, Nucl. Instrum. Methods Phys. Res. Sect. A **557**, 516 (2006).
[35] P. Friedag, Ph.D. thesis, Westfälischen Wilhelms-Universität Münster, 2013 (unpublished), http://repositorium.uni-muenster.de/document/miami/627d5ad1-6043-417b-94ba-5c87309bc2bd/diss_friedag.pdf
[36] C. Couratin *et al.*, Phys. Rev. A **88**, 041403 (2013).
[37] M. Tandecki *et al.*, Nucl. Instrum. Methods Phys. Res. Sect. A **629**, 396 (2011).
[38] E. Traykov *et al.*, Nucl. Instrum. Methods Phys. Res. Sect. A **648**, 1 (2011).
[39] D. Beck *et al.*, Hyperfine Interact. **132**, 4738 (2001).
[40] T. Porobic *et al.* [Nucl. Instrum. Methods Phys. Res., Sect. A (to be published)].
[41] S. Van Gorp *et al.*, Nucl. Instrum. Methods Phys. Res. Sect. A **638**, 192 (2011).

[42] F. Glück, Prog. Electromagn. Res. B **32**, 319 (2011); **32**, 351 (2011).
[43] COMSOL: Multiphysics Modeling and Simulation, http://www.comsol.com
[44] G. Savard *et al.*, Phys. Lett. A **158**, 247 (1991).
[45] M. Tandecki, Ph.D. thesis, Katholieke Universiteit Leuven, 2011 (unpublished), http://fys.kuleuven.be/iks/wi/files/final-version-thesis-michael-tandecki.pdf
[46] X. Fléchard (private communication).
[47] M. Beck (private communication).